You might find this additional info useful...

This article cites 44 articles, 24 of which can be accessed free at:
http://ajpheart.physiology.org/content/297/2/H512.full.html#ref-list-1

This article has been cited by 1 other HighWire hosted articles
The arrythmogenic potential of post-myocardial infarction cytokine treatment
D. J. McKitrick
Am J Physiol Heart Circ Physiol 2009; 297 (2): H508-H509.
[Full Text] [PDF]

Updated information and services including high resolution figures, can be found at:
http://ajpheart.physiology.org/content/297/2/H512.full.html

Additional material and information about *AJP - Heart and Circulatory Physiology* can be found at:
http://www.the-aps.org/publications/ajpheart

This infomation is current as of May 30, 2011.

Granulocyte colony-stimulating factor increases sympathetic reinnervation and the arrhythmogenic response to programmed electrical stimulation after myocardial infarction in rats

Tsung-Ming Lee,[1] Chien-Chang Chen,[2] and Nen-Chung Chang[3]

[1]*Cardiology Section, Department of Medicine, Taipei Medical University and Chi-Mei Medical Center, Tainan;* [2]*Cardiology Section, Department of Surgery, Chi-Mei Medical Center, Tainan; and* [3]*Cardiology Section, Department of Medicine, Taipei Medical University and Hospital, Taipei, Taiwan*

Lee TM, Chen CC, Chang NC. Granulocyte colony-stimulating factor increases sympathetic reinnervation and the arrhythmogenic response to programmed electrical stimulation after myocardial infarction in rats. *Am J Physiol Heart Circ Physiol* 297: H512–H522, 2009. First published June 5, 2009; doi:10.1152/ajpheart.00077.2009.—Granulocyte colony-stimulating factor (G-CSF) has been used for the repair of infarcted myocardium, but concerns have been raised regarding its proarrhythmic potential. We analyzed the influence of G-CSF treatment on sympathetic nerve remodeling and the expression of nestin in a rat model of experimental myocardial infarction (MI). Twenty-four hours after ligation of the anterior descending artery, male Wistar rats were randomized to receive either saline (MI/C) or G-CSF (MI/G) for 5 days. At 56 days after infarction, MI/G rats had a significantly higher left ventricular ejection fraction accompanied by a significant decrease in the left ventricular end-diastolic dimension than the MI/C group. Myocardial norepinephrine levels revealed a significant elevation in MI/G rats in the border zone compared with MI/C rats. Immunohistochemical analysis for tyrosine hydroxylase, growth-associated protein 43, and neurofilament also confirmed the changes of myocardial norepinephrine. At 5 days after infarction, MI/G rats had increased numbers of tissue-infiltrated CD34$^+$ cells, although a similar increase in circulating neutrophil counts between sham-operated rats treated with G-CSF and MI/G rats was observed. Compared with MI/C rats, MI/G rats showed an increase of nestin and nerve growth factor expression, as assessed by protein expression and mRNA levels. The arrhythmia scores during programmed stimulation were significantly higher in MI/G rats than in MI/C rats, suggesting proarrhythmic potential. These findings suggest that, although G-CSF administration after infarction improved myocardial function, it resulted in the activation of nestin and nerve growth factor expression and increased sympathetic reinnervation, which may increase the arrhythmogenic response to programmed electrical stimulation.

sympathetic nervous system; remodeling

GRANULOCYTE COLONY-STIMULATING FACTOR (G-CSF) is known to mobilize progenitor cells from the bone marrow and resident cardiac progenitor cells (4). G-CSF mobilized progenitor cells are not only capable of tissue differentiation but are also likely to regenerate the myocardium, resulting in improved cardiac function in animal and human studies (40, 41). Despite promising results of G-CSF therapy, this treatment is potentially hazardous because of the cytokine's multisystemic effects. Late-onset toxicity has been a concern as a result of nonessential cells, such as neural stem cells, incorporating into the regenerating myocardium, resulting in the generation of non-

cardiac tissues and life-threatening arrhythmias. A recent study (19) showed fatal ventricular fibrillation after G-CSF administration, and G-CSF can induce neuronal differentiation (35). Coculture of mesenchymal stem cells and neonatal rat ventricular myocytes produced an arrhythmogenic substrate that facilitated reentry (7). Pak et al. (33) demonstrated that mesenchymal stem cell injection to the swine myocardium induces increased sympathetic nerve sprouting throughout the ventricles. In contrast, others (2, 25) have recently shown that G-CSF administration 1–7 days before the induction of myocardial infarction (MI) attenuated fatal ventricular arrhythmias. However, the cytokine treatment was started before MI in these studies. Because treatment before acute MI is a virtual impossibility in most clinical situations, there has been a great deal of interest in understanding the effects of G-CSF and using it as an adjunctive treatment (starting treatment after MI) of arrhythmias.

Nerve growth factor (NGF) is a trophic factor that is critical for the differentiation, survival, and synaptic activity of the peripheral sympathetic and sensory nervous systems (39). In ischemic hearts, an increase in cardiac NGF leads to the regeneration of sympathetic nerves (5, 24). Expression of cardiac NGF correlates with the density of sympathetic innervation in the heart (36), and the amount of NGF can affect sympathetic nerve survival and synaptic transmission between neurons and cardiac myocytes (30). These results demonstrate the importance of NGF in the regulation of sympathetic innervation.

Increased sympathetic nerve density after myocardial injury has been shown to be highly associated with the occurrence of lethal arrhythmias and sudden cardiac death in humans (6). During the chronic stage of MI, a regional increase in sympathetic nerves has been commonly observed (43). Nerve fiber innervation after myocardial damage may have occurred via the mobilization of neural stem cells. During embryogenesis, the intermediate filament protein nestin (a marker of adult neural stem cells) is expressed in migrating and proliferating cells, whereas during differentiation, nestin is downregulated (44). However, after injury to muscular or neuronal tissue, nestin expression is transiently reinduced (44). Based on the postulated role of neural stem cell recruitment to damaged tissue, we assessed *1*) whether the long-term effect of G-CSF adjunctive therapy after infarction can modulate sympathetic reinnervation in a rat MI model and *2*) the role of nestin-expressing neural stem cells and NGF expression in nerve sprouting. Functional and immunohistochemical analyses were

performed on *days 5* and *56* after MI, time points reflecting the early and late phase of post-MI remodeling in rats.

METHODS

Animals. Male Wistar rats were subjected to ligation of the anterior descending artery as previously described (28), resulting in infarction of the left ventricular (LV) free wall. Animals were anesthetized with an intraperitoneal injection of ketamine (70 mg/kg). Twenty-four hours after MI, rats were randomized into groups to receive saline (MI/C group; subcutaneous administration of saline daily for 5 days) or G-CSF (MI/G group; 50 μg/kg, subcutaneous administration, Filgrastim, Kirin Brewery, Tokyo, Japan) daily for 5 days. Sham-operated (sham) rats served as controls to exclude the possibility that the drugs themselves directly alter sympathetic reinnervation. Thus, rats were assigned to the following four groups: sham, sham with G-CSF treatment (sham/G), MI/C, and MI/G. The heart was excised on *days 5* or *56* after MI as early and late remodeling of sympathetic innervation. The animal experiments were approved and conducted in accordance with local institutional guidelines for the care and use of laboratory animals in the Chi-Mei Medical Center (no. 95021301).

Echocardiography. To confirm that G-CSF administration is effective in improving of cardiac function and remodeling, transthoracic echocardiography was performed using a HP Sonos 5500 system equipped with a 15–6L probe (6–15 MHz, SONOS 5500, Philips Medical System, Best, The Netherlands) in rats under anesthesia with ketamine (90 mg/kg ip) on *days 0* and *56* as previously described (28). M-mode tracing of the LV from the parasternal long-axis view was obtained to measure the LV end-diastolic diameter dimension (LVEDD) and LV end-systolic diameter dimension (LVESD), and fractional shortening (FS; in %) was calculated.

Hemodynamics and infarct size measurements. Hemodynamic parameters and infarct size were measured on *day 56* after MI as previously described (28). Using a 2-Fr micromanometer-tipped catheter (model SPR-407, Millar Instruments, Houston, TX) inserted through the right carotid artery, we measured LV systolic and diastolic pressure as the mean of measurements from five consecutive pressure cycles. The maximal rate of the LV pressure rise ($+dP/dt$) and decrease ($-dP/dt$) was measured. After the arterial pressure measurement, rats were intubated and artificially ventilated with humidified room air supplemented with oxygen for in vivo electrophysiological experiments. After completion of the electrophysiological tests, the hearts were immediately divided into the right and left atria, right ventricles, LVs, and scarred areas. Each tissue was then weighed individually. To evaluate the degree of pulmonary edema, lungs were also weighed. It has been shown that hypertrophy of the residual myocardium progresses after infarction only if the infarct size is >30% of the LV (34). Thus, with respect to clinical importance, only rats with infarction >30% of the LV were selected for analysis.

In vivo electrophysiological experiments. To assess the potential arrhythmogenic risk of G-CSF administration, we performed in vivo programmed electric stimulation. Because the residual neural integrity at the infarct site is one of the determinants of the response to electrical induction of ventricular arrhythmias (19), only rats with a transmural scar on *day 56* after infarction were included. Body temperature was maintained at 37°C with a thermostatically controlled heating lamp. Programmed electrical stimulation was performed with electrodes sewn to the epicardial surface of the right ventricular outflow tract. Arrhythmias were induced with the Bloom stimulator. To induce ventricular arrhythmias, pacing was performed at a cycle length of 120 ms (S_1) for eight beats followed by one to three extrastimuli (S_2, S_3, and S_4) at shorter coupling intervals. The end point of ventricular pacing was the induction of ventricular tachyarrhythmia. Ventricular tachyarrhythmias, including ventricular tachycardia and ventricular fibrillation, were considered nonsustained when they lasted ≤15 beats and sustained when they lasted >15 beats. An arrhythmia scoring

system was modified as previously described (27), so that $0 =$ noninducible preparations, $1 =$ nonsustained tachyarrhythmias induced with three extrastimuli, $2 =$ sustained tachyarrhythmias induced with three extrastimuli, $3 =$ nonsustained tachyarrhythmias induced with two extrastimuli, $4 =$ sustained tachyarrhythmias induced with two extrastimuli, $5 =$ nonsustained tachyarrhythmias induced with one extrastimulus, $6 =$ sustained tachyarrhythmias induced with one extrastimulus, and $7 =$ tachyarrhythmias induced during the eight paced beats. If the heart stopped before the pacing, the arrhythmia score assigned to that heart was 8. When multiple forms of arrhythmias occurred in one heart, the highest score was used. Experimental protocols were typically completed within 10 min.

Real-time RT-PCR of nestin and NGF mRNA. Real-time quantitative RT-PCR was performed from samples obtained from the border zone (0–2 mm outside the infarct) with the TaqMan system (Prism 7700 Sequence Detection System, PE Biosystems) on *day 5* for nestin and *day 56* for NGF as previously described (28). For nestin (GenBank Accession No. NM_012987), the primers were 5′-TTTGAGGACCTAGGGACTGAGGC-3′ (sense) and 5′-CCAGAAGGCTCAGCACTGTCCTG-3′ (antisense). For NGF, the primers were 5′-TCCACCCACCCAGTCTTCCA-3′ (sense) and 5′-GCCTTCCTGCTGAGCACACA-3′ (antisense). For cyclophilin, the primers were 5′-ATGGTCAACCCCACCGTGTTCTTCG-3′ (sense) and 5′-CGTGTGAAGTCACCACCCTGACACA-3′ (antisense). Cyclophilin mRNA was chosen as the internal standard because it is expressed at a relatively constant level in virtually all tissues. For quantification, nestin and NGF expression were normalized to the expression of the housekeeping gene cyclophilin. Reaction conditions for 40 rounds of amplification were carried out.

Western blot analysis of nestin and NGF. Samples obtained from the border zone and remote zone (>2 mm outside the infarct) on *day 5* for nestin analysis and *day 56* for NGF analysis were homogenized with a kinamatic Polytron blender. Homogenates were centrifuged at 10,000 *g* for 30 min to pellet the particulate fractions. Protein (20 μg) was separated by 10% SDS-PAGE and electrotransferred onto a nitrocellulose membrane. The nitrocellulose membrane was then incubated with rabbit polyclonal anti-nestin antibody (clone rat-401, Chemicon) at 1:1,000 dilution and with rabbit polyclonal anti-NGF antibody (Chemicon) at 1:500 dilution for 2 h. Antigen-antibody complexes were detected with HRT substrate peroxide solution (Millipore, Billerica, MA). Films were volume integrated within the linear range of the exposure using a scanning densitometer. The relative abundance of nestin and NFG protein was obtained by normalizing the density of nestin and NFG protein against that of β-actin. Experiments were replicated three times, and results are expressed as mean values.

Immunohistochemical experiments of CD34, nestin, glial fibrillary acidic protein, tyrosine hydroxylase, growth-associated protein 43, and neurofilament. To investigate the spatial distribution and quantification of sympathetic nerve fibers, the analysis of immunohistochemical staining was performed on LV muscle from the border zone on *days 5* and *56*. Papillary muscles were excluded from the study because a variable sympathetic innervation has been reported (10). Because nestin may be also expressed in non-neural stem cells (13), glial fibrillary acidic protein was stained to confirm the nature of nestin$^+$ neural stem cells. The coexpression of glial fibrillary acidic protein in nestin$^+$ neural stem cells was recognized as a phenotype of neural progenitors (16). Paraffin-embedded tissues were sectioned at a thickness of 5 μm. Tissues were incubated with anti-CD34 (1:200, Santa Cruz Biotechnology, Santa Cruz, CA), anti-nestin (1:200, clone rat-401, Chemicon), anti-glial fibrillary acidic protein (1:500, Chemicon), anti-tyrosine hydroxylase (1:200, Chemicon), anti-growth-associated protein 43 (a marker of nerve sprouting, 1:400, Chemicon), and anti-neurofilament antibodies (a marker of sympathetic nerves, 1:1,000, Chemicon) in 0.5% BSA in PBS overnight at 37°C. Immunostaining was performed using a standard immunoperoxidase technique (N-Histofine Simple Stain MAX PO kit, Nichirei, Tokyo,

Japan). Immunofluorescence was used for tissues stained with nestin and glial fibrillary acidic protein. Secondary antibodies were goat anti-mouse IgG conjugated to rhodamine (1:250–1:500, Molecular Probes) and goat anti-rabbit IgG conjugated to FITC (1:500, Jackson Laboratories). Immunolabeled sections were examined through the use of confocal laser scanning microscopy (Nikon C1si, Tokyo, Japan) as previously described (29). Isotype-identical directly conjugated antibodies served as negative controls.

The slides were coded so that the investigator was blinded to the identification of the rat sections. Slides were initially scanned at low power ($\times 100$) to identify areas of intense staining. Nerve density was measured from areas of intense staining on the tracings by computerized planimetry (Image Pro Plus, Media Cybernetics, Silver Spring, MD) as previously described (29). The density of nerve fibers was quantitatively measured from 10 randomly selected fields at a magnification of $\times 400$ and expressed as the ratio of labeled nerve fiber area to total area ($n = 8$ per group). Likewise, the colocalization of nestin with glial fibrillary acidic protein fluorescence was quantitatively analyzed. For a quantitative analysis, numbers of CD34$^+$ cells were counted in at least three randomly selected fields of view in each slide ($n = 8$ per group) at a magnification of $\times 400$ in the border zone.

Laboratory measurements. To confirm the effect of G-CSF, blood samples (0.2 ml) were taken from the tail vein on *days 0, 5, 28,* and *56* after saline or G-CSF treatment ($n = 8$ per group). Blood cell counts were performed on a Coulter counter (T-660, Coulter Electronics, Hialeah, FL), and differential leukocyte counts were measured in a central laboratory by independent, experienced observers without knowledge of the group or sampling time.

Although cardiac reinnervation has been shown in immunohistochemical staining of tyrosine hydroxylase, growth-associated factor 43, and neurofilament, it did not imply that the nerves are functional. Thus, to examine the sympathetic nerve function after the administration of G-CSF, we measured LV norepinephrine levels from the border zone on *day 56* after infarction. Myocardial tissue samples were minced and suspended in 0.4 N perchloric acid with 5 mmol/l reduced glutathione (pH 7.4) and homogenized with a Polytron homogenizer for 60 s in 10 volumes. Samples were immediately centrifuged at 3,000 *g* for 10 min, and the supernatant was stored at $-70°C$ until further analysis. The supernatant protein concentration was determined using the BCA protein assay reagent kit (Pierce). Total norepinephrine levels were measured using a commercial ELISA kit (Noradrenalin ELISA, IBL Immuno-Biological Laboratories, Hamburg, Germany).

Statistical analysis. Results are presented as means $\pm$ SD. Differences among the groups were tested using one-way ANOVA. Subsequently, analysis for significant differences between the two groups was performed with a multiple-comparison test (Scheffé's method). Electrophysiological data (scoring of programmed electrical stimulation-induced arrhythmias) were compared with a Kruskal-Wallis test followed by a Mann-Whitney test. The relationships between the nestin$^+$ and glial fibrillary acidic protein$^+$ area fraction (%) and tyrosine hydroxylase-positive area fraction (%) were analyzed by Spearman correlation and multiple linear regression. The significant level was set at $P < 0.05$.

RESULTS

We found no significant differences in mortality between the two infarcted groups throughout the study (4 of 15 infarcted rats in the MI/C group and 3 of 15 infarcted rats in the MI/G group). G-CSF had little effect on cardiac gross morphology in the sham rats (Table 1). At 56 days after infarction, the infarcted area of the LV was very thin and was totally replaced by fully differentiated scar tissue. The weight of the LV inclusive of the septum remained essentially constant at 56

Table 1. *Cardiac morphology, hemodynamics, and NE levels on day 56 after MI*

	Sham	Sham/G	MI/C	MI/G
No. of rats	10	11	11	12
Body weight, g	420 ± 22	428 ± 18	415 ± 22	410 ± 16
Heart rate, beats/min	390 ± 24	418 ± 15	408 ± 20	417 ± 23
LVESP, mmHg	112 ± 6	108 ± 9	103 ± 11	104 ± 7
LVEDP, mmHg	5 ± 2	5 ± 4	$18 \pm 3^*$	$16 \pm 5^*$
+dP/dt, mmHg/s	7374 ± 516	6934 ± 392	$3009 \pm 320^*$	$3842 \pm 359^*†$
$-$dP/dt, mmHg/s	6835 ± 352	5923 ± 364	$2068 \pm 282^*$	$2795 \pm 282^*†$
Infarct size, %			41 ± 4	40 ± 3
LV weight/body weight, mg/g	2.10 ± 0.20	2.15 ± 0.18	$3.05 \pm 0.35^*$	$2.80 \pm 0.33^*$
RV weight/body weight, mg/g	0.52 ± 0.04	0.53 ± 0.08	$0.76 \pm 0.15^*$	$0.51 \pm 0.06†$
Lung weight/body weight, mg/g	4.15 ± 0.50	4.18 ± 0.39	$5.42 \pm 0.50^*$	$4.40 \pm 0.45†$
Plasma NE, ng/ml	2.7 ± 1.1	2.5 ± 1.3	$4.3 \pm 1.7^*$	$5.4 \pm 1.6^*$
Border NE, µg/g protein	1.36 ± 0.34	1.20 ± 0.39	$2.36 \pm 0.22^*$	$4.29 \pm 0.75^*†$

Values are means $\pm$ SD. Sham, sham-operated rats; sham/G, sham rats treated with granulocyte colony-stimulating factor (G-CSF); MI/C, rats with myocardial infarction (MI) treated with saline; MI/G, rats with MI treated with G-CSF; LVESP, left ventricular (LV) end-systolic pressure; LVEDP, LV end-diastolic pressure; NE, norephinephrine. *$P < 0.05$ compared with the respective sham groups; †$P < 0.05$ compared with MI/C rats.

days between the infarcted groups. Infarct size did not differ between the infarcted groups.

Hemodynamics. On *day 56* after infarction, G-CSF did not significantly affect systolic blood pressure in MI/G rats compared with MI/C rats (Table 1). +dP/dt and $-$dP/dt were significantly improved in the MI/G group on *day 56* compared with MI/C rats.

Peripheral blood cell counts. Neutrophil counts in peripheral blood are shown in Fig. 1. The neutrophil counts showed a significant increase in the G-CSF-treated groups than that in the saline groups on *day 5* and decreased thereafter. There was a similar increase in neutrophils between sham/G and MI/G rats. There were no significant changes in lymphocytes, red blood cells, or platelets throughout the experiment in the four groups (data not shown).

Echocardiography. As shown in Fig. 2, echocardiography showed a significant decrease in LVEDD and significant increases in LV FS in MI/G rats compared with MI/C rats on *day 56* after MI. These findings suggest improvements in LV remodeling and function by G-CSF treatment.

Immunohistochemical analyses. To show the extent of stem cell mobilization after G-CSF application, immunohistochemical analyses from the border zone on *day 5* were performed. As shown in Fig. 3, G-CSF promoted CD34$^+$ cell mobilization and homing to the myocardium after MI. G-CSF significantly increased the number of CD34$^+$ cells in MI/G rats on *day 5* compared with MI/C rats [12 $\pm$ 7 vs. 5 $\pm$ 4 cells/high-power field (magnification: $\times 400$), $P < 0.05$].

In the LV of sham rats, nestin-immunoreactive cells were not detected in the myocardium (data not shown). Nestin immunoreactivity was observed in the border zone on *day 5* after MI, which was associated with fiber-like structures (Fig. 3). The amount of neural stem cells coexpressing nestin$^+$ and glial fibrillary acidic protein$^+$ cells was significantly higher in MI/G rats than in MI/C rats.
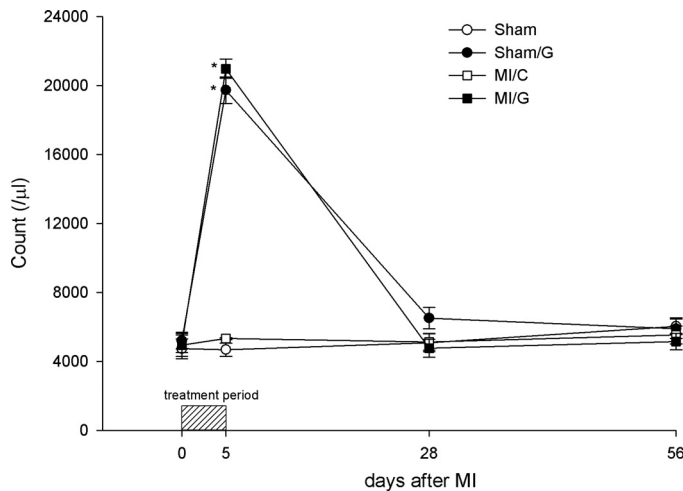
Fig. 1. Peripheral neutrophil counts at 5 days after myocardial infarction (MI). Rats were divided into the following groups: sham-operated rats (sham group), sham rats treated with granulocyte-stimulating factor (G-CSF; sham/G group), MI rats treated with saline (MI/C group), and MI rats treated with G-CSF (MI/G group). The increase of neutrophil count was greater in G-CSF-treated groups than in saline-treated groups. Data are represented as means ± SD; $n = 8$ rats/group. *$P < 0.05$ vs. sham rats and MI/C rats at the same age.

To further delineate the phenotype, the expression of the sympathetic neuronal protein tyrosine hydroxylase, growth-associated protein 43, and neurofilament was examined. On *day 5*, there were no significant quantitative differences in the area fractions of tyrosine hydroxylase$^+$ nerve fibers between the infarcted groups (data not shown). On *day 56*, the tyrosine hydroxylase$^+$ nerve area fraction was significantly larger in MI/C rats than in sham rats (Fig. 4). Furthermore, MI/G rats showed significantly larger nerve area fractions in the border zone than MI/C rats ($0.28 \pm 0.08\%$ in MI/G rats vs. $0.17 \pm 0.05\%$ in MI/C rats, $P < 0.0001$). Similar to the tyrosine hydroxylase results, the area fractions of growth-associated protein 43$^+$ and neurofilament$^+$ nerve fibers were significantly increased in MI/G rats compared with MI/C rats ($0.15 \pm 0.05\%$ in MI/G rats vs. $0.09 \pm 0.03\%$ in MI/C rats for growth-associated protein 43, $P < 0.0001$, and $0.18 \pm 0.04\%$ in MI/G rats vs. $0.07 \pm 0.02\%$ in MI/C for neurofilament, $P < 0.0001$). As shown in Fig. 5, there was a significant correlation between the nestin$^+$ and glial fibrillary acidic protein$^+$ area fraction (in %) and tyrosine hydroxylase-positive area fraction (in %) in infarcted rats ($P < 0.001$).

Western blot analysis and real-time RT-PCR of nestin and NGF. Figure 6 shows the serial changes in the myocardial protein expression of nestin. Western blot analysis showed that nestin expression levels were significantly upregulated (by 2.0-fold) in the border zone in MI/C rats compared with sham rats ($P < 0.0001$) on *day 5*. On *day 5*, compared with MI/C rats, nestin levels in MI/G rats were significantly higher in the border zone. On *day 56*, nestin protein levels returned to normal levels in the border and remote zones. Corresponding changes for nestin were obtained by immunofluorescent detection (data not shown).

Western blot analysis showed that NGF levels were significantly upregulated (by 1.8-fold) in the border zone in MI/C rats compared with sham rats ($P < 0.0001$; Fig. 7) on *day 56*. Compared with MI/C rats, NGF levels in MI/G rats were significantly higher in the border zone.

PCR amplification of cDNA revealed that nestin mRNA levels showed 2.7-fold upregulation in the border zone in MI/C rats compared with sham rats ($P < 0.0001$; Fig. 8). In MI/G rats, nestin mRNA levels were significantly increased compared with those in MI/C rats on *day 5*. The increased magnitude of nestin mRNA levels was similar to the protein level changes, implying that nestin production is a critical regulation step in nerve sprouting. Similar to the nestin mRNA change, NGF mRNA levels were significantly increased in MI/G rats compared with MI/C rats on *day 56* after infarction (Fig. 8).

Circulating and myocardial norepinephrine levels. Circulating plasma norepinephrine levels remained similar between the two infarcted groups (Table 1). Although cardiac reinnervation has been shown in immnohistochemical staining of tyrosine hydroxylase, growth-associated protein 43, and neurofilament, it did not imply that the nerves are functional. Thus, to investigate cardiac sympathetic function, we determined ventricular norepinephrine levels. G-CSF administration did not affect the basal tissue norepinephrine concentrations in the sham group. LV norepinephrine levels were significantly upregulated (by 2.02-fold) in the border zone in MI/C rats compared with sham rats (2.33 ± 0.20 vs. 1.37 ± 0.35 μg/g protein, $P < 0.0001$). Compared with MI/C rats, LV norepinephrine levels in MI/G rats were significantly higher in the border zone on *day 56*.

Electrophysiological stimulation. To further elucidate the physiological effect of the increase of sympathetic reinnervation, ventricular pacing was performed. A representative electrocardiogram record in a MI/C rat is shown in Fig. 9. The arrhythmia scores in sham rats were very low (0.2 ± 0.4). In contrast, ventricular tachyarrhythmias (consisting of ventricular tachycardia and ventricular fibrillation) were inducible by programmed stimulation in MI/C rats. The MI/G group showed a significant increase in the inducibility of ventricular tachyarrhythmias compared with the MI/C group on *day 56*.

DISCUSSION

The present study demonstrated that G-CSF recruited CD34$^+$ cells and nestin-expressing stem cells in the early stage of MI and increased NGF expression and sympathetic reinnervation in the late stage of MI. Although some improvement in ventricular function represented a positive outcome of G-CSF administration, this treatment has the potential downside of creating excessive sympathetic reinnervation that may predispose the heart to arrhythmias. These results were concordant with the effects of G-CSF, as documented structurally, by the increase in cardiac nerve sprouting, molecularly, by myocardial nestin and NGF protein expression and mRNA levels, biochemically, by tissue norepinephrine levels, and electrophysiologically, by aggravation of fatal ventricular tachyarrhythmias.

In contrast with previous studies with G-CSF, the present study demonstrates a side effect of G-CSF. The effect of G-CSF on worsening fatal arrhythmias was supported by the following lines of evidence: *1*) there was a G-CSF effect on CD34$^+$ cells and nestin expression in the early stage of MI, *2*) excessive sympathetic reinnervation was observed in the border zone in the late stage of MI (*day 56*) but not on *day 5*, and *3*) the severity of pacing-induced fatal arrhythmias was associated with the degree of sympathetic reinnervation.
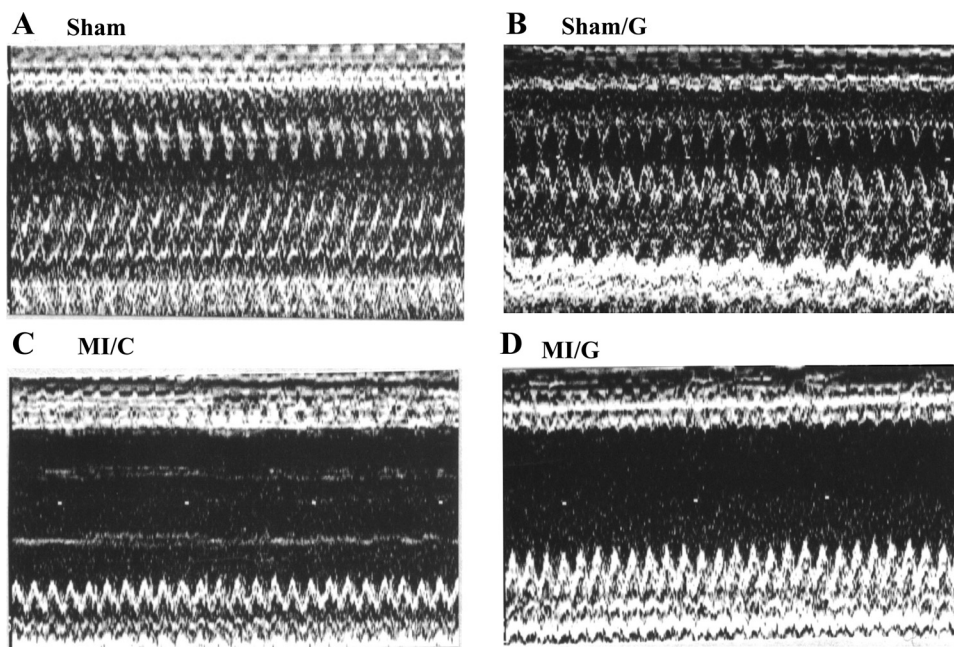
Fig. 2. *Top*, representative M-mode images on *day 56* after infarction revealed hypokinetic-to-akinetic anterior walls and left ventricular (LV) dilation in infarcted hearts in contrast to normal anterior wall motion in sham and sham/G hearts. *A*: sham; *B*: sham/G; *C*: MI/C; *D*: MI/G. *Bottom*, data represented as means $\pm$ SD; $n =$ 8 rats/group. Note the improvement of remodeling and function in MI/G compared with MI/C rats. *$P < 0.05$ compared with the respective sham groups at the same age; †$P < 0.05$ compared with MI/C rats on *day 56*.
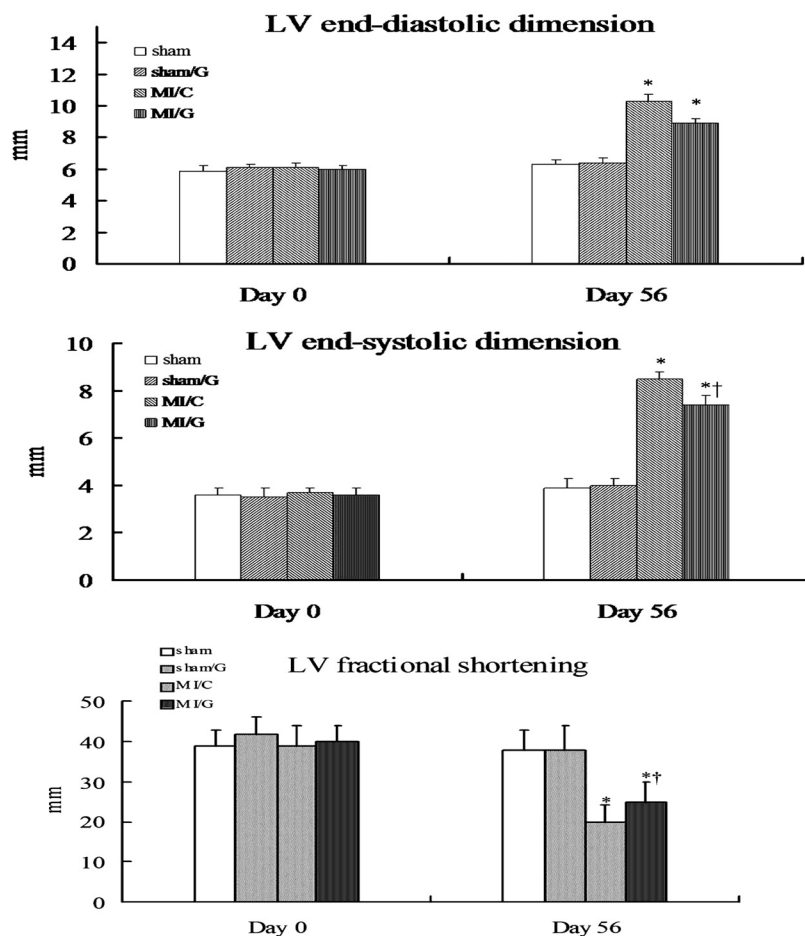
Evidence of a G-CSF effect on CD34$^+$ cells and nestin expression in the early stage of MI. On *day 5* after MI, in addition to an increase in the number of neutrophils, the most striking effect of peripheral administration of G-CSF on the myocardium was seen in the border zone, where G-CSF significantly increased the number of tissue-infiltrating CD34$^+$ cells in infarcted rats. G-CSF treatment promoted CD34$^+$ cell infiltration in the infarcted myocardium of MI rats but not in
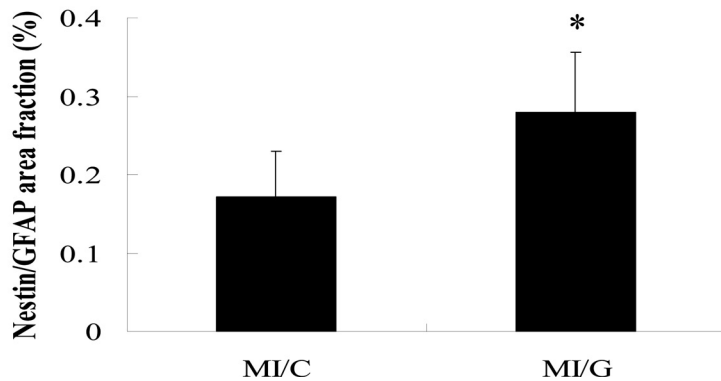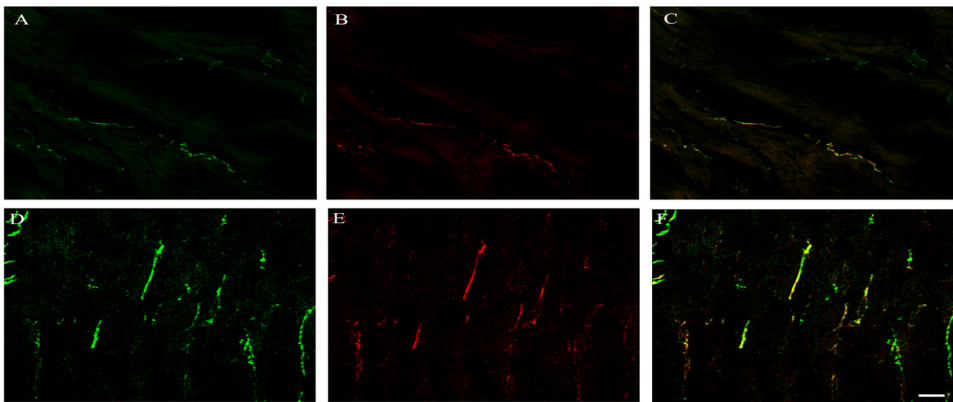
Upper Panel
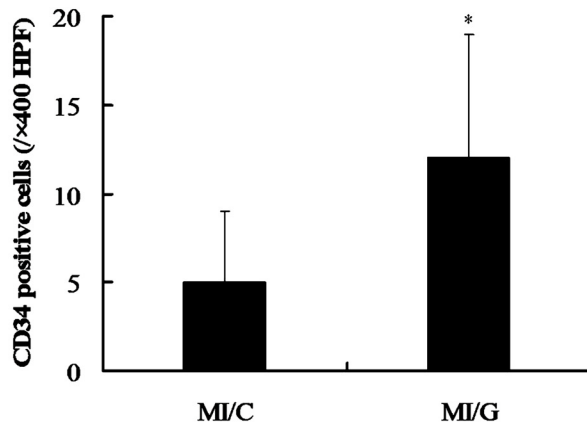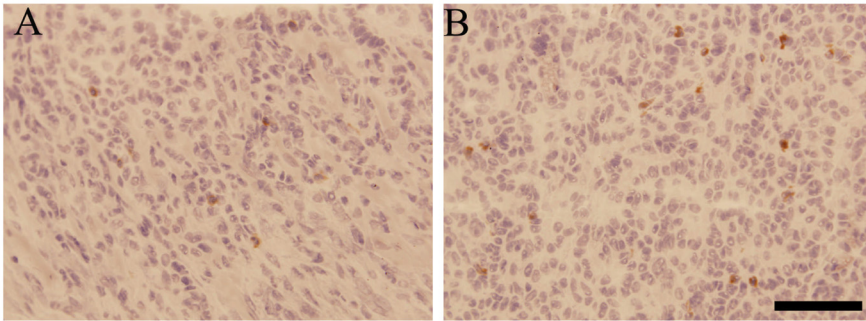
Lower Panel

Fig. 3. *Top*, representative immunohisto-chemical stainings of CD34 (brown) in the border zone at 5 days after MI. The bar graph shows the number of CD34^{+} cells in high-power fields (magnification: ×400). *A*: MI/C. *B*: MI/G. Data are represent as means ± SD; $n = 8$ rats/group. *Bottom*, glial fibrillary acidic protein expression in nestin[+] neural-like stem cells 5 days after MI. Nestin immunoreactivity (green fluorescence, *A* and *D*) in the border zone stained positively for glial fibrillary acidic protein (GFAP; red fluorescence, *B* and *E*), as reflected by the appearance of yellow fluores-cence (*C* and *F*). The area of nestin[+]-GFAP[+] expression in relation to the whole area of myocardial tissue in the field of view is shown. *A–C*: MI/C; *D–F*, MI/G. Bar = 20 μm. *$P <$ 0.05 compared with MI/C rats.
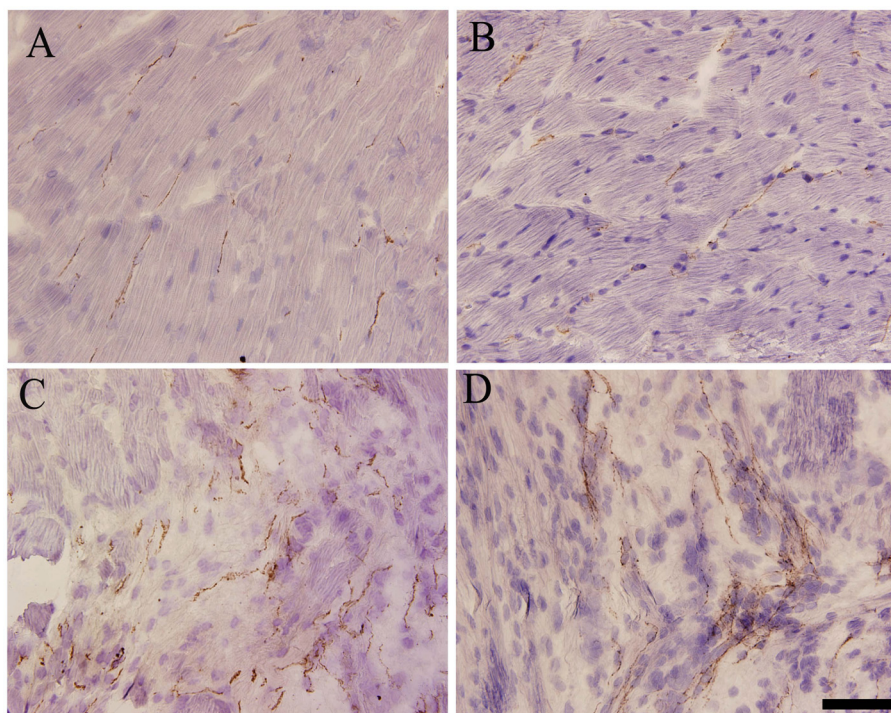
Fig. 4. Immunohistochemical staining for tyrosine hydroxylase (TH) in the border zone on *day 56* after MI (magnification: ×400). TH-positive nerve fibers (brown color) were located between myofibrils and oriented in a longitudinal direction as that of myofibrils. *A*: sham; *B*: sham/G; *C*: MI/C; *D*: MI/G. Bar = 50 μm. Data are represented as means ± SD; $n = 8$ rats/group. *$P < 0.05$ compared with sham and sham/G rats; †$P < 0.05$ compared with MI/C rats.
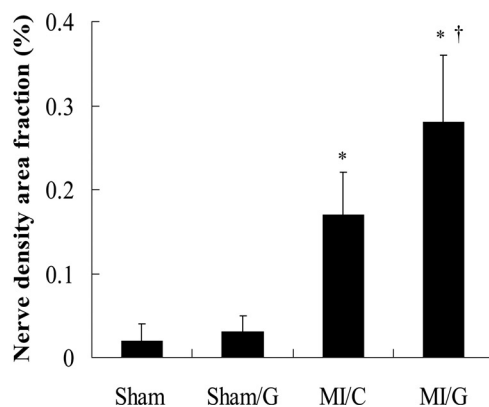
the myocardium of sham rats, despite a similar increase in the peripheral neutrophil count. Our finding was consistent with the findings of Abbott et al. (1), who showed that stem cell mobilization alone did not lead to significant engraftment of circulating cells in tissues expressing inefficiency of chemoattractant factors. Under the influence of chemoattractants, such as stromal cell-derived factor 1, that are produced in response to injury, G-CSF upregulated CXCR4 expression on CD34^{+} cells, receptors of stromal cell-derived factor 1, and promoted effective recruitment of circulating CD34^{+} cells attached to the myocardium (1).

Since we found increased mobilization and homing capacity of CD34^{+} progenitor cells, we addressed the question of if these cells may have induced nerve remodeling in the ischemic myocardium. The enriched CD34^{+} progenitor cells were paralleled by a high number of nestin^{+}-glial fibrillary acidic protein^{+} cells in the border zone. The observation was consistent with the findings of Shyu et al. (37), who showed that implanted CD34^{+} stem cells can differentiate into nestin^{+} neurons and glial fibrillary acidic protein^{+} glial cells. In infarcted rats, G-CSF plays a pivotal role in increasing the nestin expression level, which was accompanied by the induction of nestin mRNA in the border zone. Nestin is known to be involved in enhancing neuronal sprouting, synaptogenesis, and neurite outgrowth, which are indispensable for neurite extension after MI. Our results were consistent with the notion that denervation resulted in an upregulation of nestin in Schwann cells of axotomized nerves at the acute phase but diminished nestin immunoreactivity on *day 56*, when the muscle is reinnervating (15).

Excessive sympathetic reinnervation was observed in the border zone in the late stage of MI (day 56) but not at day 5. The finding was compatible with the notion that an infarcted myocardium causes a disappearance of sympathetic innervation, which is followed by a phase of excessive sympathetic reinnervation (19). Transcription and translation levels of NGF were significantly increased after the administration of G-CSF in infarcted rats. Our results were consistent with the findings of Drapeau et al. (12), who showed that neural stem cells were initially recruited to the infarct region of the damaged rat heart
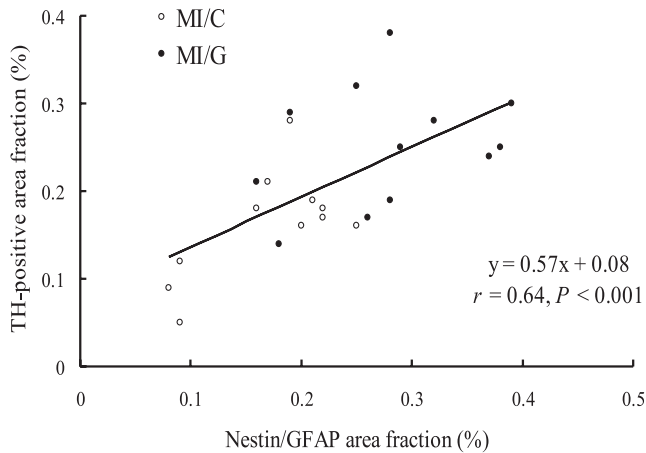
Fig. 5. Relationship between the nestin$^+$-glial fibrillary acidic protein$^+$ area fraction (in %) and TH-positive area fraction (in %) in infarcted rats. Linear regression between these two parameters is shown ($n = 23$, $r = 0.64$, $P < 0.001$).

and consequently contribute to sympathetic innervation, probably through enhancing NGF expression. As the morphological features of sympathetic reinnervation appeared to be increased at 56 days after infarction, sympathetic nerve function, as assessed by the norepinephrine content of the myocardium, showed a significant increase. Thus, the structural features of sympathetic ingrowth are established not only at anatomic impact but also at functional features of this sprouting phenomenon. G-CSF, a neuronal ligand, counteracts programmed cell death and drives neurogenesis because it acts on neurons that express G-CSF receptors (35). However, according to our results, preventing neuron apoptosis is not a mechanism by which G-CSF enhanced sympathetic reinnervation because tyrosine hydroxylase-immunoreactive fibers were similarly reduced at 5 days in infarcted rats treated with or without G-CSF.
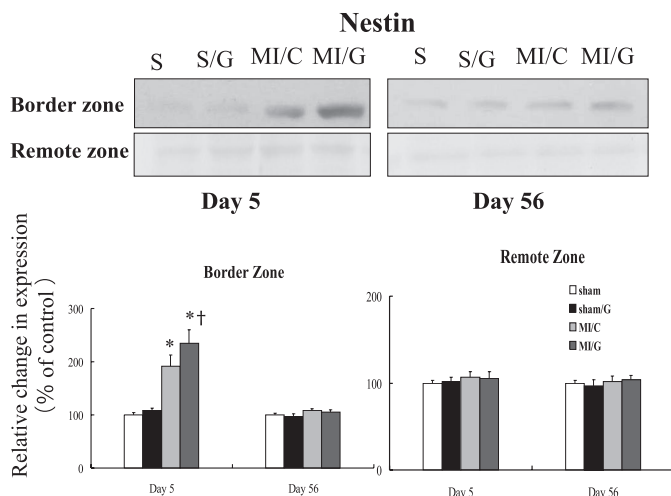

Fig. 6. Representative immunoblots showing nestin protein levels in the border zone and remote zone on *days 5* and *56* in sham (S), sham/G (S/G), MI/C, and MI/G rats. Quantified data of nestin protein expression in the border zone and remote zone are shown. Relative abundance was obtained by normalizing the density of nestin protein against that of β-actin. Results are means ± SD of 3 independent experiments; $n = 8$ rats/group. *$P < 0.05$ compared with sham and sham/G rats; †$P < 0.05$ compared with MI/C rats.
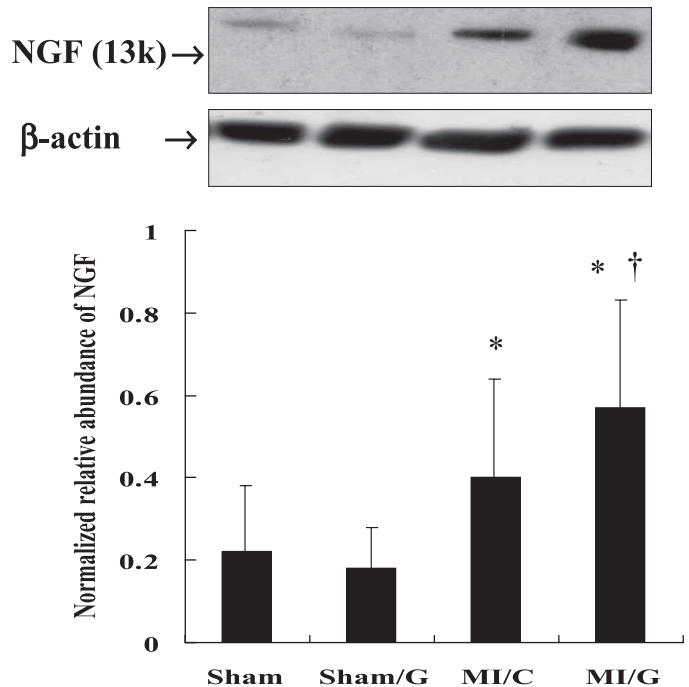

Fig. 7. Western blot analysis of nerve growth factor (NGF; molecular mass: 13 kDa) in homogenates of the LV from the border zone on *day 56*. Compared with MI/C rats, NGF levels in MI/G rats were significantly higher in the border zone by quantitative analysis. Relative abundance was obtained by normalizing the density of NGF protein against that of β-actin. Results are means ± SD of 3 independent experiments. *$P < 0.05$ compared with sham and sham/G rats; †$P < 0.05$ compared with MI/C rats.

The severity of pacing-induced fatal arrhythmias was associated with the degree of sympathetic reinnervation. Although a previous study (33) has shown that stem cell administration induced increased sympathetic nerve density, this study did not provide evidence that the nerve sprouts are destined to become hyperfunctional and to induce fatal arrhythmias. Our findings are further supported by Cao et al. (6), who showed that increased postinjury sympathetic nerve density may be responsible for the occurrence of ventricular arrhythmia and sudden cardiac death.

Although the beneficial effect of G-CSF on post-MI LV remodeling and function has been observed in several studies (18, 31, 32), controversy still exists. Previous studies (31, 32) using G-CSF alone or in combination with stem cell factor either before or immediately after MI induction in mice have reported improved function, attributing these effects to new vessel formation and decreased apoptosis of cardiomyocytes. On the other hand, Deten et al. (11) showed no functional benefits. Deten et al. (11) reported that even though c-Kit$^+$ and CD45$^-$ stem cell mobilization happens, it is not enough to bring any beneficial effect for the infarcted heart. In the present study, the administration of G-CSF showed subtle but significant improvements in physiological parameters, including hemodynamics and echocardiographic data. This discrepancy could be due to differences in protocols, species, the time point of treatment initiation, and periods of treatment. Indeed, homing of stem cells or even the access of G-CSF itself to the infarcted region of the myocardium is impaired when the coronary artery is permanently occluded and G-CSF is administered after coronary ligation.
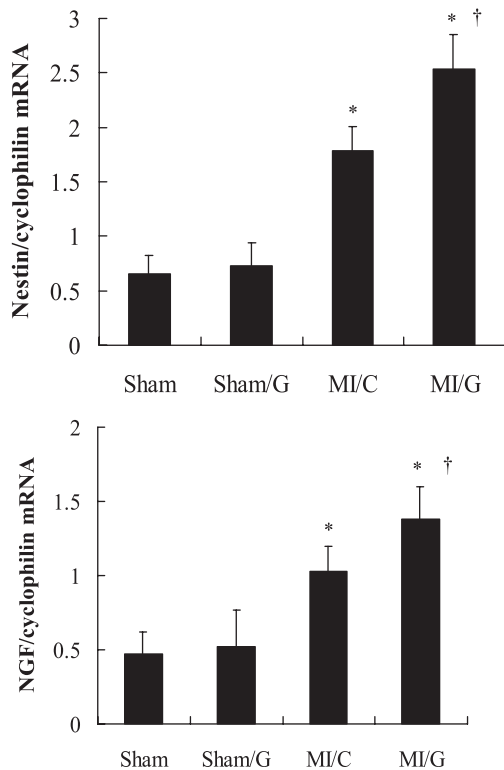
Fig. 8. LV nestin mRNA levels in the border zone on *day 5* after MI and NGF mRNA levels in the border zone on *day 56* after MI. Each mRNA was corrected for the mRNA level of cyclophilin. Cyclophilin mRNA levels served as the internal standard. All samples were run in triplicate. Data are represented as means ± SD; $n = 8$ rats/group. *$P < 0.05$ compared with sham and sham/G rats; †$P < 0.05$ compared with MI/C rats.

Other mechanisms. Although the present study suggests that the mechanisms of enhanced G-CSF-induced sympathetic reinnervation and proarrhythmia are related to increased nestin expression, other potential mechanisms need to be studied, such as paracrine/autocrine effects and cardiac fibrosis. First, G-CSF may directly activate VEGF signals. VEGF has been shown to stimulate neurite outgrowth in retinal ganglion cell cultures (3) and cerebral cortical neurons (23) via VEGF receptor 2. Second, G-CSF exacerbated cardiac fibrosis (8), thereby inducing the risk of isolated regional slowing of conduction and reentrant arrhythmias.

Study limitations. There are some limitations to the present study that have to be acknowledged. First, we used the small size of the rat heart to our advantage to quantify the changes of nerve sprouting after MI. Although rats offer an incredibly valuable tool for the study of post-MI remodeling, it is essential to be aware of differences that exist between animal models and human disease. We must bear in mind that the results obtained in the experimental animals may not translate directly to humans. The drug effect of permanent coronary occlusion in the rat model and late patency of the infarcted-related artery in most clinical settings on the development of sympathetic reinnervation may be different. Furthermore, coronary artery ligation in the rat usually results in a large transmural infarct size (average: 40%), which contrasts to MI in humans. Second, recent technological developments in echocardiography have facilitated the analysis of ventricular remodeling and heart function after the induction of MI in small laboratory animals,

but there are limitations compared with human echocardiography. Mainly, LV dimensions were estimated either from one-dimensional M-mode tracings (38), area measurements in parasternal views (9), or volume calculations from single cross sections (14). These methods have been validated in humans, but it is generally recognized that the accuracy of the prolate-ellipse, area-length, and truncated ellipsoid methods is limited to normally shaped and sized ventricles, whereas the biplane method of disks is accurate in abnormally shaped ventricles (26). Due to the small heart size, the high heart rate, and technical limitations, delineation of endocardial borders in rats is conventionally not possible in apical views. Indeed, the M-mode used in this study is the most common measurement of LV remodeling and function after infarction in rats. Third, the source and phenotype of the progenitor cell that gave rise to nestin-expressing neural stem cells in the border zone remain presently undefined. The normal heart may contain a reservoir of resident cardiac progenitor cells (42) that, after damage, differentiate to a neural stem cell phenotype. Either residing cardiac stem cells or bone marrow stem cells might migrate to the infarct site and differentiate to neural progenitor
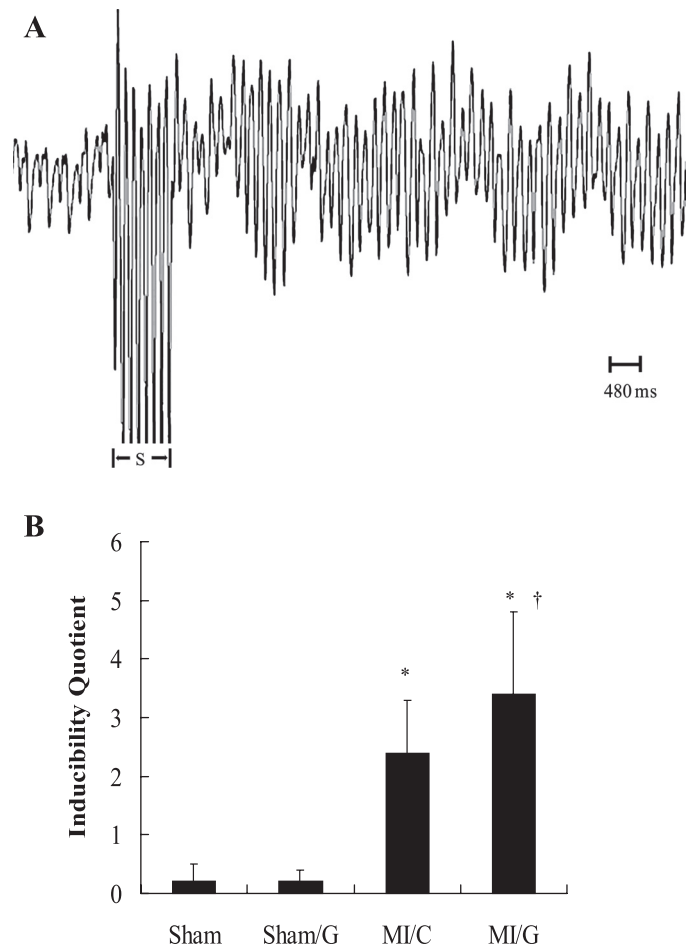

Fig. 9. *Top*: representative sustained ventricular arrhythmias induced by ventricular pacing in a sham rat. After eight basic stimuli (S) at a cycle length of 120 ms, sustained ventricular tachyarrhythmias were observed (score: 7). *Bottom*: inducibility quotient of ventricular arrhythmias by programmed electrical stimulation at 56 days after MI in an in vivo model. Results are means ± SD; $n = 9$ rats/group. *$P < 0.05$ compared with sham and sham/G rats; †$P < 0.05$ compared with MI/C rats.

cells (17). Finally, it is unknown whether nestin-expressing cells are necessarily destined to become functional neurons or simply exhibit ectopic expression of such markers as part of an injury response. Nestin expression was also detected in pancreatic stem cells, endothelial cells during active angiogenesis, and myocardium-derived c-Kit$^+$ progenitor cells (22). Whether they would eventually express mature neuronal markers, such as neuronal nuclear antigen-positive and microtubule-associated protein 2, remains to be determined. The enhanced expression of tyrosine hydroxylase and tissue norepinephrine levels in the myocardium could reflect the increased production of norepinephrine from nerve sprouting of mature sympathetic neurons.

Conclusions. These data show that G-CSF was associated with mobilization of CD34$^+$ cells and increases of nestin and NGF expression and played an important role in the sympathetic reinnervation within the infarcted myocardium. These effects are functionally and structurally important because they are linked to increased severity of fatal arrhythmias. Further studies, including a longer-term observation, are needed to more conclusively address the effectiveness and safety of G-CSF therapy.

REFERENCES

1. **Abbott JD, Huang Y, Liu D, Hickey R, Krause DS, Giordano FJ.** Stromal cell-derived factor-1alpha plays a critical role in stem cell recruitment to the heart after myocardial infarction but is not sufficient to induce homing in the absence of injury. *Circulation* 110: 3300–3305, 2004.
2. **Baldo MP, Davel AP, Nicoletti-Carvalho JE, Bordin S, Rossoni LV, Mill JG.** Granulocyte colony-stimulating factor reduces mortality by suppressing ventricular arrhythmias in acute phase of myocardial infarction in rats. *J Cardiovasc Pharmacol* 52: 375–380, 2008.
3. **Böcker-Meffert S, Rosenstiel P, Röhl C, Warneke N, Held-Feindt J, Sievers J, Lucius R.** Erythropoietin and VEGF promote neural outgrowth from retinal explants in postnatal rats. *Invest Ophthalmol Vis Sci* 43: 2021–2026, 2002.
4. **Brunner S, Huber BC, Fischer R, Groebner M, Hacker M, David R, Zaruba MM, Vallaster M, Rischpler C, Wilke A, Gerbitz A, Franz WM.** G-CSF treatment after myocardial infarction: impact on bone marrow-derived vs cardiac progenitor cells. *Exp Hematol* 36: 695–702, 2008.
5. **Cao JM, Chen LS, KenKnight BH, Ohara T, Lee MH, Tsai J, Lai WW, Karagueuzian HS, Wolf PL, Fishbein MC, Chen PS.** Nerve sprouting and sudden cardiac death. *Circ Res* 86: 816–821, 2000.
6. **Cao JM, Fishbein MC, Han JB, Lai WW, Lai AC, Wu TJ, Czer L, Wolf PL, Denton TA, Shintaku IP, Chen PS, Chen LS.** Relationship between regional cardiac hyperinnervation and ventricular arrhythmias. *Circulation* 101: 1960–1969, 2000.
7. **Chang MG, Tung L, Sekar RB, Chang CY, Cysyk J, Dong P, Marbán E, Abraham MR.** Proarrhythmic potential of mesenchymal stem cell transplantation revealed in an in vitro coculture model. *Circulation* 113: 1832–1841, 2006.
8. **Cheng Z, Ou L, Liu Y, Liu X, Li F, Sun B, Che Y, Kong D, Yu Y, Steinhoff G.** Granulocyte colony-stimulating factor exacerbates cardiac fibrosis after myocardial infarction in a rat model of permanent occlusion. *Cardiovasc Res* 80: 425–434, 2008.
9. **Coatney RW.** Ultrasound imaging: principles and applications in rodent research. *ILAR J* 42: 233–247, 2001.
10. **Dahlstrom A.** Observations on the accumulation of noradrenaline in the proximal and distal parts of peripheral adrenergic nerves after compression. *J Anat* 99: 677–689, 1965.
11. **Deten A, Volz HC, Clamors S, Leiblein S, Briest W, Marx G, Zimmer HG.** Hematopoietic stem cells do not repair the infarcted mouse heart. *Cardiovasc Res* 65: 52–63, 2005.
12. **Drapeau J, El-Helou V, Clement R, Bel-Hadj S, Gosselin H, Trudeau LE, Villeneuve L, Calderone A.** Nestin-expressing neural stem cells identified in the scar following myocardial infarction. *J Cell Physiol* 204: 51–62, 2005.
13. **El-Helou V, Dupuis J, Proulx C, Drapeau J, Clement R, Gosselin H, Villeneuve L, Manganas L, Calderone A.** Resident nestin$^+$ neural-like cells and fibers are detected in normal and damaged rat myocardium. *Hypertension* 46: 1219–1225, 2005.
14. **Francis J, Weiss RM, Wei SG, Johnson AK, Felder RB.** Progression of heart failure after myocardial infarction in the rat. *Am J Physiol Regul Integr Comp Physiol* 281: R1734–R1745, 2001.
15. **Friedman B, Zaremba S, Hockfield S.** Monoclonal antibody rat 401 recognizes Schwann cells in mature and developing peripheral nerve. *J Comp Neurol* 295: 43–51, 1990.
16. **Fukuda S, Kato F, Tozuka Y, Yamaguchi M, Miyamoto Y, Hisatsune T.** Two distinct subpopulations of nestin-positive cells in adult mouse dentate gyrus. *J Neurosci* 23: 9357–9366, 2003.
17. **Hao HN, Zhao J, Thomas RL, Parker GC, Lyman WD.** Fetal human hematopoietic stem cells can differentiate sequentially into neural stem cells and then astrocytes in vitro. *J Hematother Stem Cell Res* 12: 23–32, 2003.
18. **Harada M, Qin Y, Takano H, Minamino T, Zou Y, Toko H, Ohtsuka M, Matsuura K, Sano M, Nishi J, Iwanaga K, Akazawa H, Kunieda T, Zhu W, Hasegawa H, Kunisada K, Nagai T, Nakaya H, Yamauchi-Takihara K, Komuro I.** G-CSF prevents cardiac remodeling after myocardial infarction by activating the Jak-Stat pathway in cardiomyocytes. *Nat Med* 11: 305–311, 2005.
19. **Hasan W, Jama A, Donohue T, Wernli G, Onyszchuk G, Al-Hafez B, Bilgen M, Smith PG.** Sympathetic hyperinnervation and inflammatory cell NGF synthesis following myocardial infarction in rats. *Brain Res* 1124: 142–154, 2006.
20. **Herre JM, Wetstein L, Lin YL, Mills AS, Dae M, Thames MD.** Effect of transmural versus nontransmural myocardial infarction on inducibility of ventricular arrhythmias during sympathetic stimulation in dogs. *J Am Coll Cardiol* 11: 414–421, 1988.
21. **Hüttmann A, Dührsen U, Stypmann J, Noppeney R, Nückel H, Neumann T, Gutersohn A, Nikol S, Erbel R.** Granulocyte colony-stimulating factor-induced blood stem cell mobilisation in patients with chronic heart failure. Feasibility, safety and effects on exercise tolerance and cardiac function. *Basic Res Cardiol* 101: 78–86, 2006.
22. **Kawada H, Takizawa S, Takanashi T, Morita Y, Fujita J, Fukuda K, Takagi S, Okano H, Ando K, Hotta T.** Administration of hematopoietic cytokines in the subacute phase after cerebral infarction is effective for functional recovery facilitating proliferation of intrinsic neural stem/progenitor cells and transition of bone marrow-derived neuronal cells. *Circulation* 113: 701–710, 2006.
23. **Khaibullina AA, Rosenstein JM, Krum JM.** Vascular endothelial growth factor promotes neurite maturation in primary CNS neuronal cultures. *Dev Brain Res* 148: 59–68, 2004.
24. **Kreusser MM, Buss SJ, Krebs J, Kinscherf R, Metz J, Katus HA, Haass M, Backs J.** Differential expression of cardiac neurotrophic factors and sympathetic nerve ending abnormalities within the failing heart. *J Mol Cell Cardiol* 44: 380–387, 2008.
25. **Kuwabara M, Kakinuma Y, Katare RG, Ando M, Yamasaki F, Doi Y, Sato T.** Granulocyte colony-stimulating factor activates Wnt signal to sustain gap junction function through recruitment of beta-catenin and cadherin. *FEBS Lett* 581: 4821–4830, 2007.
26. **Lang RM, Bierig M, Devereux RB, Flachskampf FA, Foster E, Pellikka PA, Picard MH, Roman MJ, Seward J, Shanewise J, Solomon S, Spencer KT, St John Sutton M, Stewart W.** Recommendations for chamber quantification. *Eur J Echocardiogr* 7: 79–108, 2006.
27. **Lee TM, Chen CC, Lin MS, Chang NC.** Effect of endothelin receptor antagonists on ventricular susceptibility in postinfarcted rats. *Am J Physiol Heart Circ Physiol* 294: H1871–H1879, 2008.
28. **Lee TM, Lin MS, Chang NC.** Effect of ATP-sensitive potassium channel agonists on ventricular remodeling in healed rat infarcts. *J Am Coll Cardiol* 51: 1309–1318, 2008.
29. **Lee TM, Lin MS, Chou TF, Tsai CH, Chang NC.** Adjunctive 17β-estradiol administration reduces infarct size by altered expression of canine myocardial connexin43 protein. *Cardiovasc Res* 63: 109–117, 2004.

30. **Lockhart ST, Turrigiano GG, Birren SJ.** Nerve growth factor modulates synaptic transmission between sympathetic neurons and cardiac myocytes. *J Neurosci* 17: 9573–9582, 1997.

31. **Ohtsuka M, Takano H, Zou Y, Toko H, Akazawa H, Qin Y, Suzuki M, Hasegawa H, Nakaya H, Komuro I.** Cytokine therapy prevents left ventricular remodeling and dysfunction after myocardial infarction through neovascularization. *FASEB J* 18: 851–853, 2004.

32. **Orlic D, Kajstura J, Chimenti S, Limana F, Jakoniuk I, Quaini F, Nadal-Ginard B, Bodine DM, Leri A, Anversa P.** Mobilized bone marrow cells repair the infarcted heart, improving function and survival. *Proc Natl Acad Sci USA* 98: 10344–10349, 2001.

33. **Pak HN, Qayyum M, Kim DT, Hamabe A, Miyauchi Y, Lill MC, Frantzen M, Takizawa K, Chen LS, Fishbein MC, Sharifi BG, Chen PS, Makkar R.** Mesenchymal stem cell injection induces cardiac nerve sprouting and increased tenascin expression in a swine model of myocardial infarction. *J Cardiac Electrophysiol* 14: 841–848, 2003.

34. **Pfeffer JM, Pfeffer MA, Fletcher PJ, Braunwald E.** Progressive ventricular remodeling in rat with myocardial infarction. *Am J Physiol Heart Circ Physiol* 260: H1406–H1414, 1991.

35. **Schneider A, Krüger C, Steigleder T, Weber D, Pitzer C, Laage R, Aronowski J, Maurer MH, Gassler N, Mier W, Hasselblatt M, Kollmar R, Schwab S, Sommer C, Bach A, Kuhn HG, Schäbitz WR.** The hematopoietic factor G-CSF is a neuronal ligand that counteracts programmed cell death and drives neurogenesis. *J Clin Invest* 115: 2083–2098, 2005.

36. **Shelton DL, Reichardt LF.** Expression of the nerve growth factor gene correlates with the density of sympathetic innervation in effector organs. *Proc Natl Acad Sci USA* 81: 7951–7955, 1984.

37. **Shyu WC, Lin SZ, Chiang MF, Su CY, Li H.** Intracerebral peripheral blood stem cell (CD34^{+}) implantation induces neuroplasticity by enhancing beta1 integrin-mediated angiogenesis in chronic stroke rats. *J Neurosci* 26: 3444–3453, 2006.

38. **Sjaastad I, Sejersted OM, Ilebekk A, Bjornerheim R.** Echocardiographic criteria for detection of postinfarction congestive heart failure in rats. *J Appl Physiol* 89: 1445–1454, 2000.

39. **Snider WD.** Functions of the neurotrophins during nervous system development: what the knockouts are teaching us. *Cell* 77: 627–638, 1994.

40. **Stamm C, Westphal B, Kleine HD, Petzsch M, Kittner C, Klinge H, Schümichen C, Nienaber CA, Freund M, Steinhoff G.** Autologous bone-marrow stem-cell transplantation for myocardial regeneration. *Lancet* 361: 45–46, 2003.

41. **Strauer BE, Brehm M, Zeus T, Köstering M, Hernandez A, Sorg RV, Kögler G, Wernet P.** Repair of infarcted myocardium by autologous intracoronary mononuclear bone marrow cell transplantation in humans. *Circulation* 106: 1913–1918, 2002.

42. **Toma JG, Akhavan M, Fernandes KJ, Barnabé-Heider F, Sadikot A, Kaplan DR, Miller FD.** Isolation of multipotent adult stem cells from the dermis of mammalian skin. *Nat Cell Biol* 3: 778–784, 2001.

43. **Vracko R, Thorning D, Frederickson RG.** Fate of nerve fibers in necrotic, healing, and healed rat myocardium. *Lab Invest* 63: 490–501, 1990.

44. **Wiese C, Rolletschek A, Kania G, Blyszczuk P, Tarasov KV, Tarasova Y, Wersto RP, Boheler KR, Wobus AM.** Nestin expression-a property of multi-lineage progenitor cells? *Cell Mol Life Sci* 61: 2510–2522, 2004.